Domain structure of epitaxial $SrRuO_3$ thin films on miscut (001) $SrTiO_3$ substrates

J. C. Jiang, W. Tian, and X. Q. Pan[a)]
Department of Materials Science & Engineering, The University of Michigan, Ann Arbor, Michigan 48109

Q. Gan and C. B. Eom
Department of Mechanical Engineering and Materials Science, Duke University, Durham, North Carolina 27708

(Received 29 January 1998; accepted for publication 27 March 1998)

The microstructure of epitaxial $SrRuO_3$ thin films grown on vicinal (001) $SrTiO_3$ substrates with miscut angle of 1.9° and miscut direction of 12° away from [100] direction was studied using transmission electron microscopy (TEM). Cross-section as well as plan-view TEM studies revealed that these films are single domain with the in-plane epitaxial orientation relationship of $SrRuO_3$[001]//$SrTiO_3$[010] and $SrRuO_3$[110]//$SrTiO_3$[100]. This result is in contrast to the previous studies of the $SrRuO_3$ thin films grown on exactly (001) $SrTiO_3$, which are composed of two types of [110] domains with nearly the same volume fraction. The occurrence of these different domain structures is attributed to the step-flow growth of the film on the substrate surface due to the miscut. © *1998 American Institute of Physics.* [S0003-6951(98)00523-3]

$SrRuO_3$ is a conductive magnetic oxide, which is paramagnetic at room temperature[1] and ferromagnetic below 160 K.[2] Recently, epitaxial thin films of $SrRuO_3$ have attracted considerable attention because of its important electrical and magnetic properties, such as high-perpendicular remnant magnetization and large magneto-optical constant[3] which make this material very useful for making various electronic and optic devices. Furthermore, $(Pb,Zr)TiO_3$ ferroelectric and $BaSrTiO_3$ high dielectric constant capacitors with $SrRuO_3$ thin film electrodes exhibit superior fatigue and leakage characteristics.[4,5] Epitaxial $SrRuO_3$ thin films have been successfully grown on different substrates by different methods, such as 90° off-axis sputtering,[6] molecular beam epitaxy,[7] and pulsed laser ablation.[8]

$SrRuO_3$ thin films grown on (001) $SrTiO_3$ and (001) $LaAlO_3$ substrates have different magnetic properties. For example, thin films formed on (001) $SrTiO_3$ and (001) $LaAlO_3$ show different coercive behavior at low temperature,[3] and thin films grown on miscut (001) $SrTiO_3$ substrate show a strong anisotropic magnetoresistance, whereas those grown on (001) $LaAlO_3$ substrate show identical magnetoresistance behavior in two orthogonal directions.[9] It is well known that the properties of perovskite oxide devices depend strongly on the surface morphology and the microstructure of the thin films. Therefore, a major challenge in heteroepitaxial perovskite devices is to explore the growth mechanisms in order to produce high quality epitaxial thin films. The deposition conditions and the choice of substrates play a key role in determining the microstructure and the properties of the thin films, thus, making it possible to deliberately control the surface morphology, domain structure, and properties of thin films.

$SrRuO_3$ has a $GdFeO_3$ type pseudo-cubic perovskite structure.[10] At room temperature, it is an orthorhombic phase with the space group of Pbnm (No. 62) and lattice parameters $a=5.5670$ Å, $b=5.5304$ Å, and $c=7.8446$ Å.[11] All the planes and directions of $SrRuO_3$ referred to in this work are based on the orthorhombic unit cell. $SrTiO_3$ has a cubic perovskite structure with the space group of Pm3m and lattice constant of $a=3.905$ Å.[12] When $SrRuO_3$ is deposited on (001) $SrTiO_3$ substrate, the film can grow epitaxially with its (001), (110), or (110) planes parallel to the $SrTiO_3$ (001) surface. Therefore, there are six possible domain structures based on the possible interfacial structural models of $SrRuO_3$/$SrTiO_3$ as shown schematically in Fig. 1. For clarity, the pseudo-cubic perovskite unit cell of $SrRuO_3$ is shown in the figure with orthorhombic indexing of the unit cell directions. The $SrRuO_3$ film can grow with its (110) plane parallel to the $SrTiO_3$ (001) surface with an in-plane orientation relationship with respect to the $SrTiO_3$ substrate of either $SrRuO_3$[001]//$SrTiO_3$[010] and $SrRuO_3$[110]//$SrTiO_3$[100] (mode X), or $SrRuO_3$[001]//$SrTiO_3$[100] and $SrRuO_3$[110]//$SrTiO_3$[010] (mode Y). The $SrRuO_3$ film can also grow with its (110) plane parallel to the (001) surface of $SrTiO_3$ with an in-plane orientation relationship of either $SrRuO_3$[001]//$SrTiO_3$[010] and $SrRuO_3$[110]//$SrTiO_3$[100] (mode X'), or $SrRuO_3$[001]//$SrTiO_3$[100] and $SrRuO_3$[110]//$SrTiO_3$[010] (mode Y'). It is also possible that the $SrRuO_3$ film grows along its [001] axis normal to the (001) surface of $SrTiO_3$, with an in-plane orientation

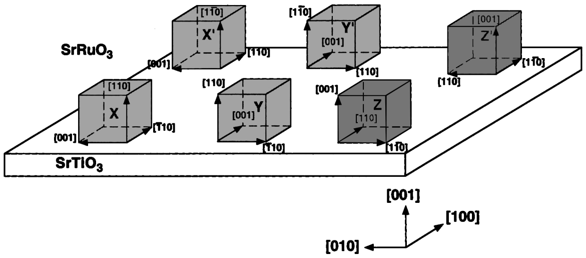

FIG. 1. Schematic diagram showing six possible growth modes of $SrRuO_3$ thin film on the (001) substrate of $SrTiO_3$. Note that while the pseudo-cubic perovskite unit cell of $SrRuO_3$ is drawn, the cell directions are indexed based on the orthorhombic unit cell.

[a)] Electronic mail: panx@engin.umich.edu relationship of either $SrRuO_3$[100]//$SrTiO_3$[110] and $SrRuO_3$[010]//$SrTiO_3$[110] (mode Z), or $SrRuO_3$ [100]//$SrTiO_3$ [110] and $SrRuO_3$ [010]//$SrTiO_3$ [110] (mode Z'). If the above six growth modes are simultaneously formed during the process of film growth, then the six domain structures will coexist in one thin film. Among the six types of domains in the film, $X(X')$-, $Y(Y')$-, and $Z(Z')$-type domains can be distinguished by means of conventional transmission electron microscopy (TEM), while the difference between the X (Y or Z) and X' (Y' or Z') is not distinguishable by the same techniques due to the pseudo-cubic characteristic of the $SrRuO_3$ structure. In the present work, we only classify the domains as three types (X, Y, and Z).

In order to investigate the effect of substrate miscut on domain structures and properties, $SrRuO_3$ thin films were grown on (001) $SrTiO_3$ substrates with different miscut angles and directions and studied by a variety of analytical methods, such as x-ray diffraction and atomic force microscopy.[13,14] In our previous work, we reported the microstructure of $SrRuO_3$ thin films on exact (001) $SrTiO_3$ substrates.[15] It was found that $SrRuO_3$ thin films grown on exact (001) $SrTiO_3$ consist of both the X- and the Y-type domains with nearly the same volume fraction. In this letter, we report the TEM studies of the $SrRuO_3$ thin films on a vicinal (001) $SrTiO_3$ substrates.

$SrRuO_3$ thin films on a vicinal (001) $SrTiO_3$ substrate, with a miscut angle (α) of 1.9° and miscut direction (β) of 12° away from the in-plane [100] direction, were deposited by 90° off-axis sputtering. Here α is defined as the angle between the surface normal and the crystallographic [001] direction of $SrTiO_3$, while β is defined as the angle between the projection of the surface normal onto the (001) plane and the in-plane [100] direction.[13]

The cross-sectional slices for TEM studies were obtained by cutting the $SrRuO_3/SrTiO_3$ heterostructural samples along the [100] direction of $SrTiO_3$ and then gluing the cut slides face-to-face by joining the $SrRuO_3$ surfaces. Plan-view and cross-section TEM specimens were prepared by mechanical grinding, polishing, and dimpling, followed by Ar-ion milling at 5 kV. Electron diffraction patterns and dark-field images were recorded in a Philips CM12 electron microscope operated at 120 kV in the EMAL at the University of Michigan.

Figure 2(a) is a dark-field image of a cross-sectional sample, formed by the (111) reflection of a $SrRuO_3$ film, viewed along the [010] direction of $SrTiO_3$. Similar to the previous TEM observations of the $SrRuO_3$ thin film grown on exact (001) $SrTiO_3$ substrate,[15] the film studied in this work has a smooth surface and a sharp interface between the film and the substrate and maintains a uniform thickness of about 100 nm over the entire specimen. The occurrence of bright and dark parts in the image indicates that the film consists of two types of domains. Figures 2(b) and 2(c) are selected area electron diffraction (SAED) patterns taken from the two $SrRuO_3$ domains of different types [corresponding to the regions marked A and B in Fig. 2(a)], for which the electron beam direction is parallel to the [010] axis of $SrTiO_3$. Figure 2(b) is identified to be the [110] zone electron diffraction pattern of $SrRuO_3$. According to this diffraction pattern, the (110) plane of the film is parallel to the (001) surface of $SrTiO_3$, while the [001] direction of the $SrRuO_3$ film lies in the film plane, indicating a Y-type domain structure in this region. In contrast, Fig. 2(c) is the [001] zone electron diffraction pattern of $SrRuO_3$, in which the (110) plane is parallel to the $SrTiO_3$ (001) surface, while the [110] direction lies in the film plane, indicating an X-type domain structure. The TEM studies of cross-sectional specimens cutting from different region of the same film revealed that the film grown on the vicinal (001) $SrTiO_3$ substrates mainly consists of the X-type domain and that the small Y-type domains only occasionally be observed.

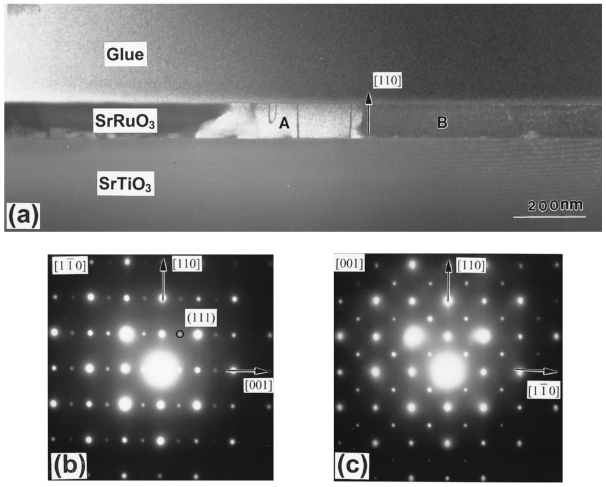

FIG. 2. (a) Dark-field image formed by the (111) reflection of $SrRuO_3$ showing two types of domain structures (bright and dark). (b) and (c) SAED patterns from the bright and dark regions showing the [110] and [001] zone of $SrRuO_3$, respectively.

The microstructure and the size distribution of X and Y types of domains in the film were investigated in plan-view samples of the same film. Micrographs in Figs. 3 and 4 were taken from different areas of the same plan-view specimen. Figure 3(a) is a SAED pattern showing the [110] zone electron diffraction patterns of the $SrRuO_3$ film. Figure 3(b) is a dark-field image formed using a weak reflection marked by ''X'' in Fig. 3(a). Comparing the diffraction pattern in Fig. 3(a) with the electron diffraction pattern of the $SrTiO_3$ substrate, it has been found that the specimen area in Fig. 3(b) has a crystallographic orientation of the X-type domain structure shown in Fig. 1. From detailed TEM studies of plane-view specimens prepared from different parts of the same $SrRuO_3$ film, it can be concluded that the X-type domains in the $SrRuO_3$ film form a continuous matrix with a small amount of islands of either Y- or Z-type domains. This is shown in Fig. 4. Figure 4(a) shows a SAED pattern taken from the same plan-view specimen as in Fig. 3. It is a superposition of SAED patterns generated from domains of all the three types shown in Fig. 1. The weak reflection marked by ''X'', ''Y'', and ''Z'' in Fig. 4(a) belong to domains of X, Y, and Z type, respectively. Figures 4(b), 4(c), and 4(d) are dark-field images formed by these three weak reflections, respectively. The white contrast in Fig. 4(b) represent X-type domains, while the black contrast represent the mixture of Y- and Z-type domains, which are bright in Figs. 4(c) and 4(d), respectively. The fine dark lines in Figs. 3(b) and 4(b) are antiphase boundaries of $SrRuO_3$. It should be pointed out that the Y- and Z-type domains were only occasionally ob-

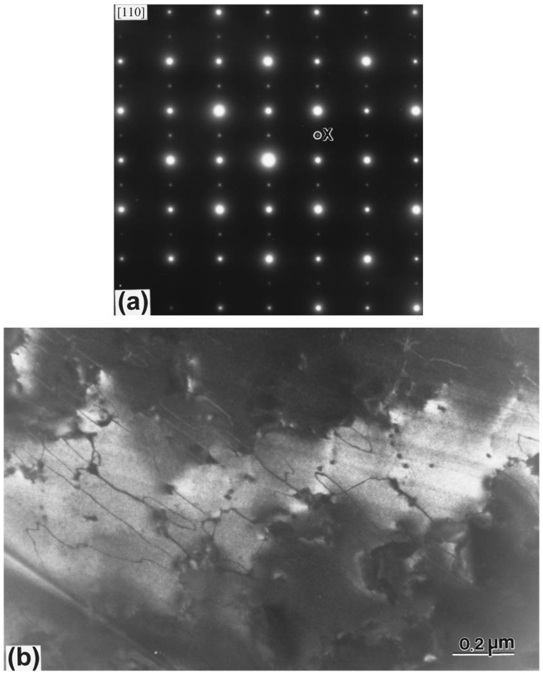

FIG. 3. (a) SAED pattern from a plan-view specimen showing [110] zone of $SrRuO_3$. (b) Dark-field image using weak reflection marked by ''X'' in (a), showing one purely X-type domain.

served. However, the previous x-ray diffraction studies using a four-circle diffractometer[13] showed that the as-grown film on the vicinal (001) $SrTiO_3$ substrate consists of a single domain (the X-type domain) structure. The reason for this inconsistency is so far unclear, based on the present studies.

The present TEM investigations of the $SrRuO_3$ thin films deposited on the vicinal (001) $SrTiO_3$ show that the film consists of a matrix domain of the X-type with some small islands of the other-type domains. The previous TEM investigations[15] showed that the $SrRuO_3$ thin films grown on exact (001) $SrTiO_3$ substrate are composed of both X- and Y-type domains with nearly the same volume fraction. The volume fraction of X-, Y-, and Z-type domains presented in the $SrRuO_3$ films grown on exact and vicinal (001) $SrTiO_3$ substrates is summarized in Table I, based on the TEM observations. The different domain structures observed in the $SrRuO_3$ thin films grown on the exact and vicinal (001) $SrTiO_3$ substrates reveal that the surface morphology of the substrate has a strong effect on the $SrRuO_3$ thin film growth. This effect may be ascribed to the influence of the periodic step-terrace structure of the miscut substrate surface on the growth mechanism of the film.[13] However, the understanding of the underlying mechanisms, such as preferential formation of a particular kind of domain structure needs further detailed studies on the microstructure of the films grown on substrates with different miscut angles and directions, and especially the study of films grown at different deposition conditions such as growth temperature, growth rate, cooling rate, and oxygen pressure.

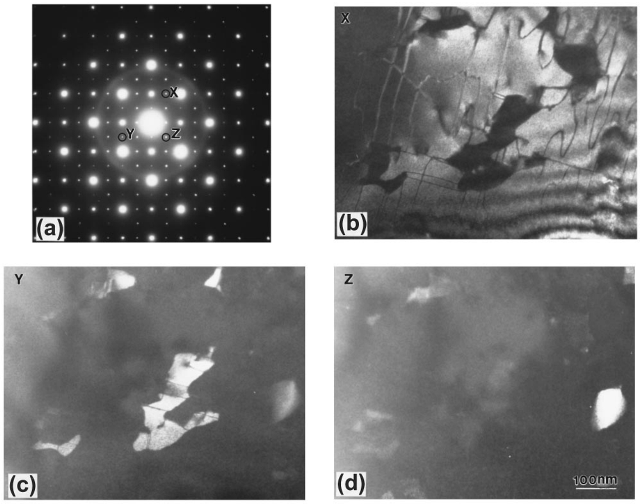

FIG. 4. (a) SAED pattern from the same plan-view specimen as that shown in Fig. 3. (b), (c), and (d) dark-field images using X, Y, and Z reflections, respectively, showing small amount of Y- and Z-type domains existing as islands within the dominant X-type domain.

TABLE I. The volume fraction of X-, Y-, and Z-type domains in the $SrRuO_3$ films grown on exact and vicinal (001) $SrTiO_3$ substrates.

Substrate orientation	X-domain (vol. %)	Y-domain (vol. %)	Z-domain (vol. %)
Exact (001)	$\sim 50\%$	$\sim 50\%$	0
Vicinal (001)	$>95\%$	$<5\%$	$\ll 1\%$

In conclusion, the $SrRuO_3$ thin films deposited by 90° off-axis sputtering on the vicinal (001) $SrTiO_3$ show a different domain structure compared to those grown on exact (001) $SrTiO_3$ substrate. The film on miscut (001) $SrTiO_3$ substrate consists of some small regions of Y- and Z-type domains embedded in a matrix domain which has the X-type domain orientation. These studies reveal that a miscut of the (001) $SrTiO_3$ substrate along the [100] direction has a strong influence on the microstructure of the $SrRuO_3$ film. Further studies of domain configurations and interfacial atomistic structures of thin films grown at different conditions are necessary to understand the underlying mechanisms of the effect.

This work was supported by the College of Engineering, the University of Michigan, Ann Arbor, Michigan.

[1] R. J. Bouchard and J. L. Gillson, Mater. Res. Bull. **7**, 873 (1972).
[2] A. Callaghan, C. W. Moller, and R. Ward, Inorg. Chem. **5**, 1572 (1966).
[3] L. Klein, J. S. Dodge, T. H. Geballe, A. Kapitulnik, A. F. Marshall, L. Antognazza, and K. Char, Appl. Phys. Lett. **66**, 2427 (1995).
[4] C. B. Eom, R. B. Van Dover, J. M. Phillips, D. J. Werder, J. H. Marshall, C. H. Chen, R. J. Cava, R. M. Fleming, and D. K. Fork, Appl. Phys. Lett. **63**, 2570 (1993).
[5] Ferroelectric Thin Films VI, edited by R. Treece, R. Jones, S. B. Desu, C. M. Foster, and I. Yoo, MRS Fall Meeting Proceeding No. 493 (Materials Research Society, Pittsburgh, 1997).
[6] C. B. Eom, R. J. Cava, R. M. Fleming, J. M. Philips, R. B. van Dover, J. H. Marshall, J. W. P. Hsu, J. J. Krajewski, and W. F. Peck, Science **258**, 258 (1992).
[7] C. Ahn, Ph.D. thesis, Stanford University, 1996.
[8] X. D. Wu, S. R. Foltyn, R. C. Due, and R. E. Muenchausen, Appl. Phys. Lett. **62**, 2434 (1993).
[9] D. B. Kacedon, R. A. Rao, and C. B. Eom, Appl. Phys. Lett. **71**, 1724 (1997).
[10] S. Geller, J. Chem. Phys. **24**, 1236 (1956).
[11] C. W. Jones, P. D. Battle, P. Lightfoot, and W. T. A. Harrison, Acta Crystallogr., Sect. C: Cryst. Struct. Commun. **C45**, 365 (1989).
[12] W. Bensch, H. W. Schmalle, and A. Reller, Solid State Ionics **43**, 171 (1990).
[13] Q. Gan, R. A. Rao, and C. B. Eom, Appl. Phys. Lett. **70**, 1962 (1997).
[14] R. A. Rao, Q. Gan, and C. B. Eom, Appl. Phys. Lett. **71**, 1171 (1997).
[15] J. C. Jiang, X. Q. Pan, and C. L. Chen, Appl. Phys. Lett. **72**, 909 (1998).